JOURNAL OF GEOPHYSICAL RESEARCH, VOL. 97, NO. C8, PAGES 12,569–12,584, AUGUST 15, 1992

The Upper Layer Circulation of the Black Sea: Its Variability as Inferred From Hydrographic and Satellite Observations

TEMEL OGUZ

Institute of Marine Sciences, Middle East Technical University, İçel, Turkey

PAUL E. LA VIOLETTE

Mississippi State University Research Center, Stennis Space Center

UMIT UNLUATA

Institute of Marine Sciences, Middle East Technical University, İçel, Turkey

Quasi-synoptic hydrographic data and satellite imagery are used to describe the circulation and the structural variability of the Black Sea with particular emphasis on the Turkish coast. The circulation is indicated to involve a variable cyclonic circulation with no apparent central locus and a well-defined cyclonic "Rim Current" containing meanders and interacting eddy fields confined to the shelf slope. Interspersed between the coastal eddies are filaments and intense jets, often with dipole eddies at their termina. The extension of these features across the shelf-slope into the central basin offshore waters implies important dynamical processes related to the shelf–deep basin exchanges. These features are often steered by the topography and evolve continuously through the mixed baroclinic-barotropic instability of the Rim Current.

1. INTRODUCTION

The Black Sea possesses a basin-wide cyclonic boundary circulation driven by the curl of the wind stress field and further modified by thermohaline fluxes and bathymetry. While knowledge of the mean circulation has advanced considerably since the first systematic studies of *Knipovich* [1932], *Neumann* [1942], and *Caspers* [1957] (Figure 1*a*), a coherent description of the general and mesoscale circulations is lacking. Based on a study of limited set of satellite imagery similar to the infrared image in Figure 1*b*, *Unluata and La Violette* [1990] indicated that the flow in the sea has strong temporal and mesoscale variability with complex interrelated eddy-dominated circulation especially prevalent in the continental shelf and slope region. However, most studies describe the flow field by its synoptic and seasonal variabilities [e.g., *Bogatko et al.*, 1979; *Blatov et al.*, 1984; *Eremeev et al.*, 1991] with little emphasis on the structural details, complexity, and variability of associated dynamics indicated by the satellite data.

Recent ship observations have been made along the Turkish coast of the Black Sea aimed at alleviating some of these deficiencies [*Oguz et al.*, 1991]. During 1987–1989, the Turkish ship R/V *Bilim* of the Middle East Technical University's Institute of Marine Sciences conducted four hydrographic surveys on the continental shelf and slope with limited extension into the deep interior. In addition, satellite data were collected to observe fine details of the spatial and temporal variability of the circulation.

In this paper we describe the principal features of the circulation of the Black Sea based on an analyses of these hydrographic and satellite data. Although our analysis will focus on the Turkish coast (where we have the most densely packed hydrological data), our aim is to show the overall relationship between the shelf-slope and central circulations. As we wish to define areas and approaches of future research into the dynamics of the Black Sea, our discussion will be qualitative rather than quantitative. We have organized the paper as follows: Section 2 presents a brief account of the present understanding of oceanographic characteristics of the Black Sea, section 3 describes the mesoscale variability and observed structure of the circulation inferred from R/V *Bilim* hydrographic data, and section 4 gives details inferred from satellite data. We discuss our results and present our conclusions in sections 5 and 6, respectively.

2. GENERAL CHARACTERISTICS

The Black Sea, with a surface area of approximately 4.2×10^5 km^2, constitutes one of the world's largest inland basins exhibiting anoxic conditions below a thin layer (~100 m) of oxygenated surface waters. To the north, the sea is connected via the Kerch Strait with the Sea of Azov. To the southwest, the sea is connected to the Aegean Sea via the Bosphorus and Dardanelles straits and the Sea of Marmara. It is through these southwest passages that the water exchanges between the Mediterranean and Black seas take place. The low-salinity waters of the Black Sea, formed as a result of an excess of runoff and precipitation over evaporation, are transported to the Mediterranean as a surface flow. Below this surface flow, saltier Mediterranean water flows northward as an undercurrent into the Black Sea. Both layers interact with each other in their north and south passages with the result, as far as the Black Sea is concerned, that the Mediterranean water enters the sea less salty (~22 psu) than when it started its passage at the Aegean end of the Dardanelles (~38 psu) [*Unluata et al.*, 1990].

Paper number 92JC00812.
0148-0227/92/92JC-00812$05.00

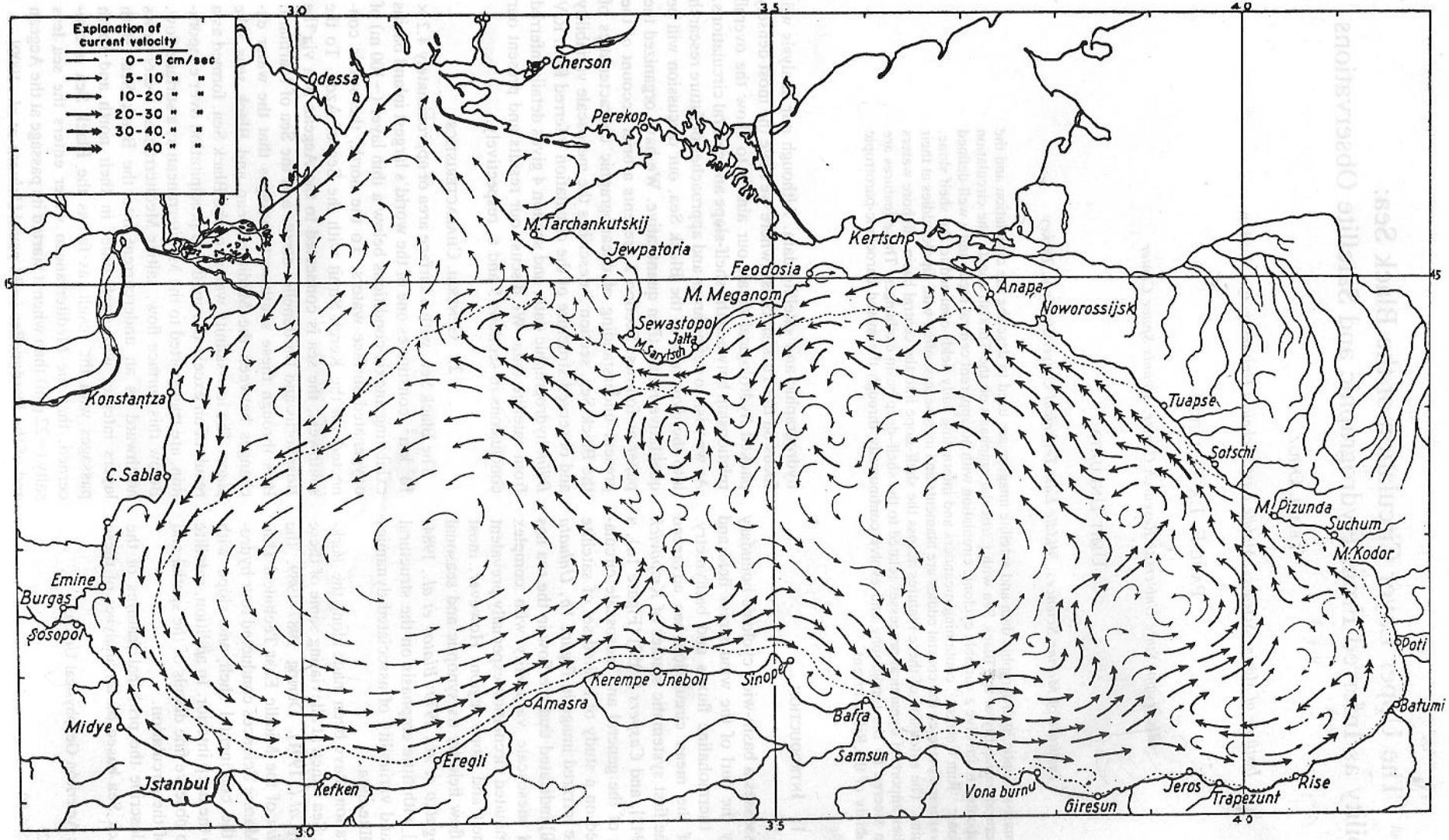

Fig. 1*a*

Fig. 1. (*a*) The summer circulation of the Black Sea [*Neumann*, 1942]. (*b*) NOAA AVHRR channel 4 (thermal) image of the Black Sea for December 18, 1989. In this image and in the other thermal imagery presented in this study, the darker areas are the colder radiated temperatures of the scene (areas that are completely black are clouds); lighter areas are warmer temperatures. The details of this synoptic thermal view (and by inference the circulation pattern) can be compared with the historical depiction of the Black Sea circulation based on sparse ship data in Figure 1*a*. The distribution of eddies and filaments shows the interrelationship and continuity of the circulation and their strong association with the shelf and slope of the Black Sea. Details of the circulation associated with the shelf and the deeper structure can be seen by comparing the thermal imagery to the bathymetric chart in Figure 2.

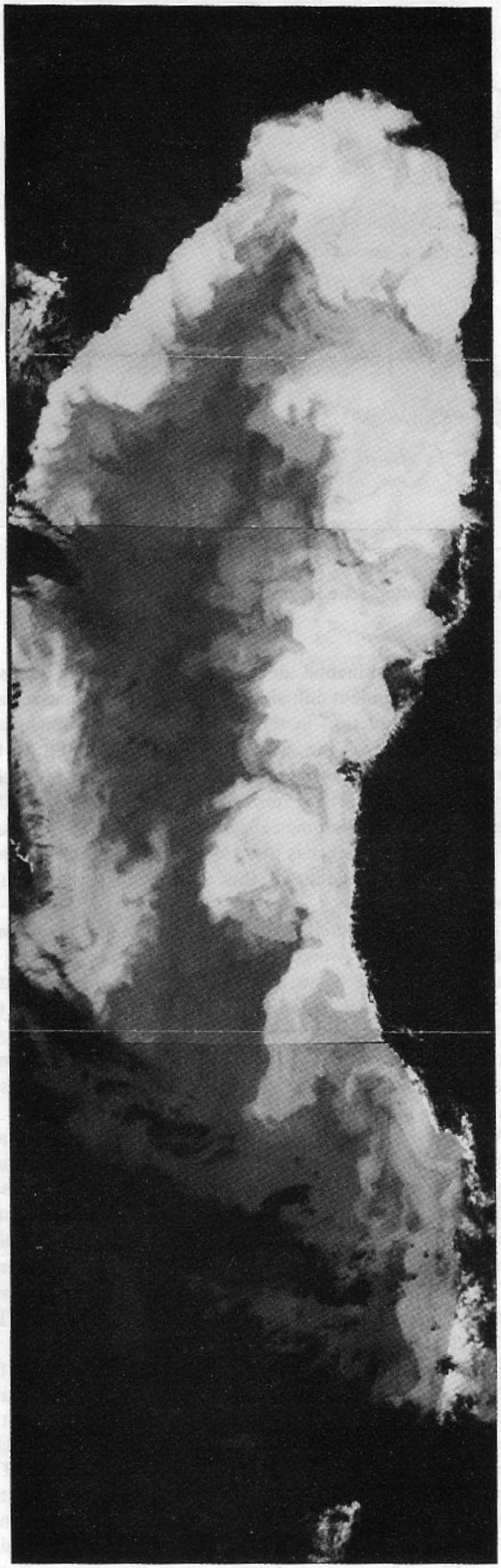

Fig. 1b

A number of studies [*Tolmazin*, 1985*b*; *Yuce*, 1990; *Latif et al.*, 1991; *Oguz and Rozman*, 1991; *Ozsoy et al.*, 1991] have described how the Mediterranean underflow enters the Black Sea, disperses on the shelf adjacent to the Bosphorus, and eventually sinks along the continental slope.

Even a casual glance at these and other past studies shows that the topography of the Black Sea basin exercises strong control on its circulation (for example, compare Figures 1 and 2). The basin's interior, with 60% of the sea's volume, has a relatively flat topography and is ~2000–2100 m deep. The shelf region (i.e., the area shallower than 200 m) that forms the periphery of the basin is generally narrow and characterized by a complex topography, with the northwestern part of the sea having the only major shelf region. Off the Turkish coast the shelf is relatively narrow, with the shelf-slope break found only 10–20 km offshore and the slope dropping to 2000 m in a distance of about another 20 km. The shelf-slope topography along the southern and southeastern coast is intersected by numerous submarine canyons.

Previous studies [e.g., *Marchuk et al.*, 1975; *Moskalenko*, 1976; *Blatov et al.*, 1984; *Bulgakov and Korotaev*, 1987; *Stanev*, 1988, 1989, 1990; *Eremeev et al.*, 1991] show that the peripheral current flows in a band 40–80 km wide. In this paper we consider this peripheral flow as a distinct current system, calling it the "Rim Current" (the dynamic reason for this distinct terminology is detailed in the discussion section). The current speed is reported to reach 40 cm/s in the upper layer, decreasing ~50% toward 100 m. At deeper levels, it decreases gradually to less than 10 cm/s. Between 500 and 1000 m the average speed is ~2.5 cm/s [*Titov*, 1985].

The aforementioned studies indicate significant seasonal differences in the circulation in the sea. During winter, strong persistent winds are said to favor the development of a strong composite flow with one elongated east-west eddy covering the basin. *Blatov et al.* [1984] state that upward motion in the central basin is compensated by downward motion at the periphery of the sea. Conversely, the summer circulation is described as having a weaker flow with two separate cyclonic gyre systems in the central basin.

The seasonal variations of the Black Sea are well shown in the historical sea surface temperature data [*Altman et al.*, 1987]. Figure 3 shows that the mean seasonal temperature variation of the entire basin follows a fairly smooth sinusoidal curve with the coldest temperatures (~7.5°C) occurring in February–March and the warmest (~24°C) in July–August.

The hydrographic data sets are not as plentiful as the historical sea surface temperature, and what data are available have typical station spacing of 80–100 km [*Blatov et al.*, 1984]. Figure 1 is typical of the circulation derived from these widely-spaced data. In turn, such simplistic maps gave rise to coarse-resolution numerical models (see, for example, the review by *Oguz et al.* [1990]). Relatively few hydrographic data in the literature indicate that the basin circulation is not as simple as these early analyses show. These few, however, show a sea with mesoscale features with much shorter spatial scales of the order of the internal Rossby radius of deformation (20–25 km) [e.g., *Fashchuk and Ayzatullin*, 1986; *Latun*, 1990].

The Black Sea possesses a pronounced two-layer haline stratification with comparatively small but important variations in each layer. The general stratification characteristics have been described by *Oguz et al.* [1991] and *Murray et al.*

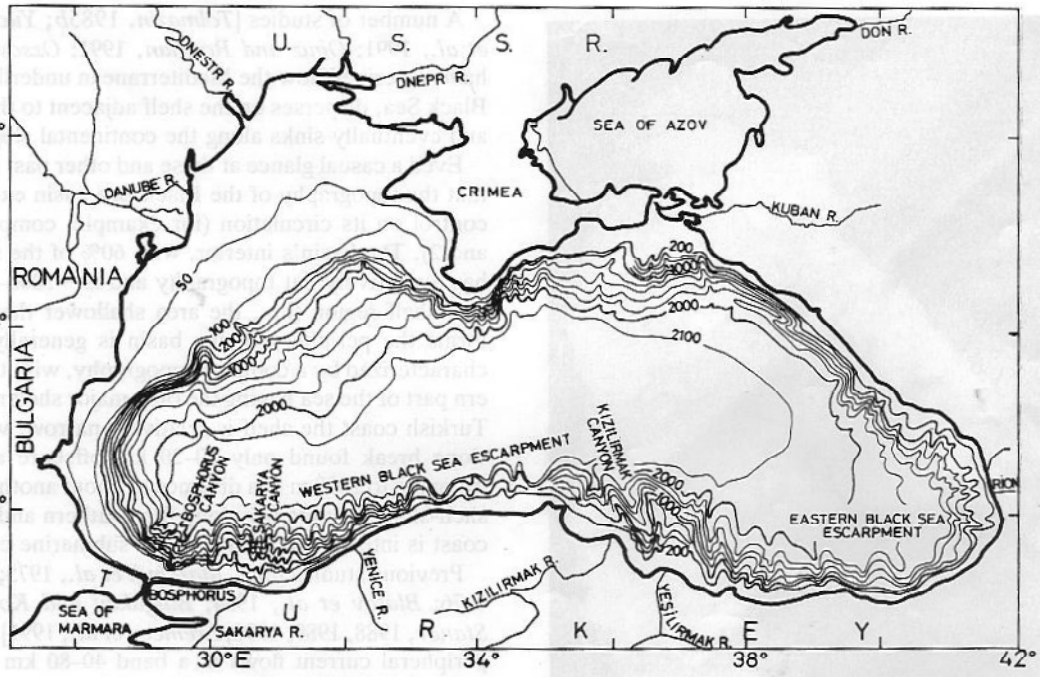

Fig. 2. The bathymetry of the Black Sea basin. Depth contours are labeled in meters.

[1991] and is typified by the sample cruise-averaged station data in Figure 4 taken from the 1987–1989 R/V *Bilim* surveys. The upper layer, maintained by a mixing of the resident water mass with an excess of fresh river water inflow, extends down to 150 m. The first 30–40 m of this layer is exposed to considerable seasonal temperature and salinity variations and overlies the permanent halocline located between depths of 50 and 150 m. In the 30- to 40-m surface layer the salinity is typically 18.0 psu, varying seasonally as much as 0.5–1.0 psu (as a result of changes in evaporation, precipitation, runoff, etc.). Within the halocline, the salinity varies $\pm 0.3 \sim 19.5$ psu at 75 m, $\pm 0.5 \sim 20.0$ psu at 100 m, and $\pm 0.3 \sim 20.5$ psu at 125 m.

The distinguishing feature of the upper layer is the Cold Intermediate Water (CIW), identified by temperatures of <8°C. CIW is said to principally form in the northwestern shelf region [*Tolmazin*, 1985*a*], and within the upper layer in the central part of the sea [*Ovchinnikov and Popov*, 1987; *Paramonov et al.*, 1988]. During winter the seasonally cold (<6°–7°C) surface waters are periodically exposed to the cooling and evaporative processes of wintertime outbreaks of cold, dry continental air masses. These events intensify the vertical turbulent diffusive and convective processes and subsequent reduction in the vertical density gradient and homogenization of the water column. The result is the formation of a homogeneously cold, dense water mass that covers the entire northwestern shelf area of the sea as well as the centers of the cyclonic cells within the interior of the sea. In none of the literature is there a reference to the buoyancy or displacement effects of this seasonally formed water mass.

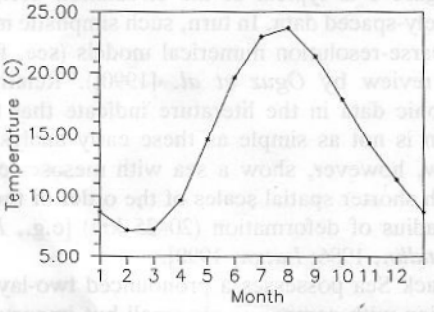

Fig. 3. The monthly variation of climatological mean sea surface temperature of the Black Sea using data compiled by *Altman et al.* [1987].

The CIW is advected by the Rim Current and maintained within the coastal waters throughout the year. During its course around the basin, it is entrapped by the associated eddy field, where it is continuously modified. At times the CIW extends into, and mixes with, the central waters. As we shall show in sections 3 and 4, this exchange with the interior is accomplished via filaments which extend from the coastal waters into the interior.

With the advent of spring and summer heating, the surface temperature warms and the CIW becomes topped by a warm surface layer that becomes more pronounced as the season progresses. The result is that the CIW is found as a subsurface temperature minimum below the seasonal thermocline that develops at 25- to 30-m depth in late spring and summer (Figure 4*a*). In turn, this spring–summer thermocline hinders the downward flux of heat into the CIW, and the CIW is therefore preserved without significant modification.

In autumn, sea surface temperatures decrease and the water column cools. The seasonal thermocline gradually weakens with increased vertical transports of heat and salt to the layer of CIW. In winter this may be further reinforced by the convective mixing in the central parts of the basin. The January 1989 cruise-averaged temperature profile for the eastern Black Sea shown in Figure 4*a* displays the presence of a 70- to 80-m-deep mixed layer with the temperature value of ~7.5°C. This layer is formed when the mixing of the

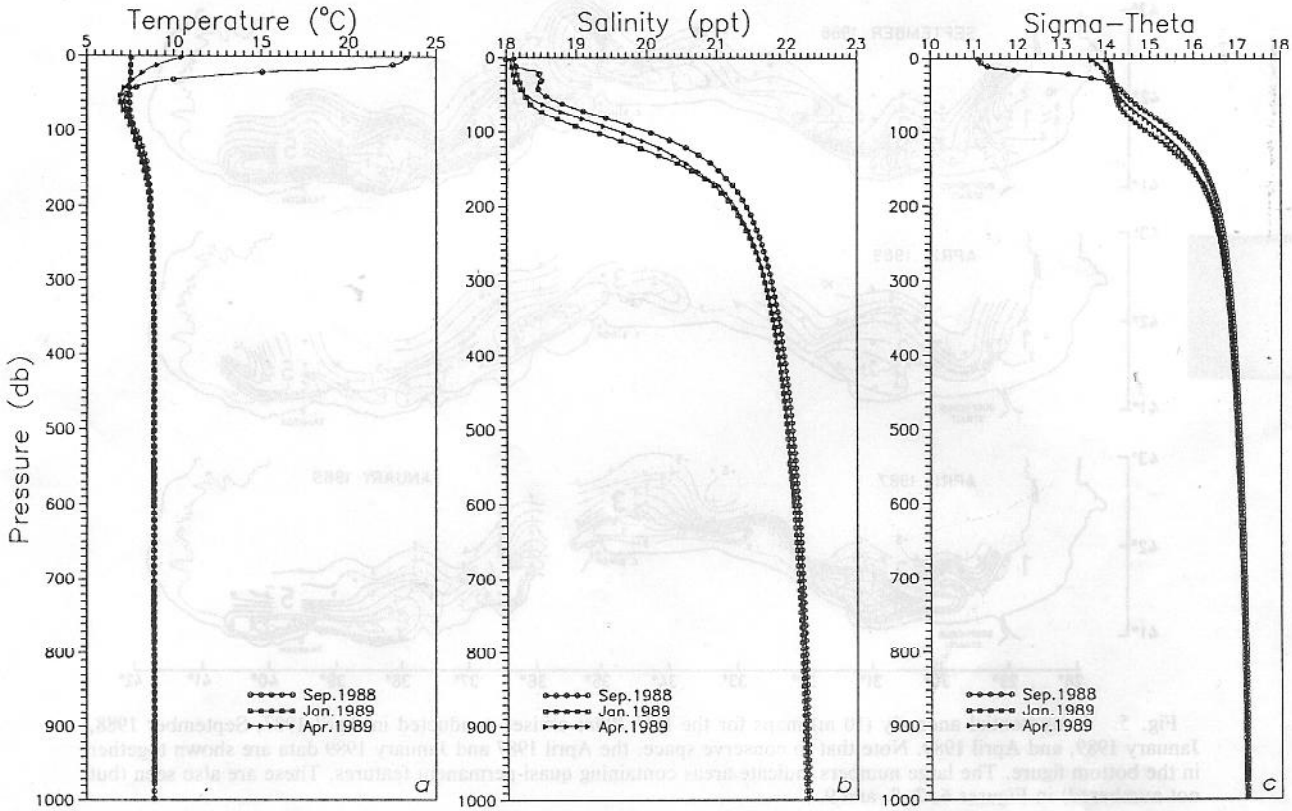

Fig. 4. Vertical profiles of (*a*) temperature, (*b*) salinity, and (*c*) density representing summer, winter, and spring conditions using spatially averaged data obtained from the September 1988, January 1989, and April 1989 cruises.

seasonally cooled surface waters of ~7°–8°C penetrates the deeper levels (~50 m) where the remnant of CIW has similar temperature values. A homogeneous layer is formed with temperatures of 7°–7.5°C down to depths of 70–80 m. A similar homothermal layer of CIW is observed during winter with cooler temperatures of ~6°C along the Turkish coast of the western Black Sea [*Oguz et al.*, 1991].

The water masses below the halocline possess almost no seasonal variation. In the layer extending from 150 m to 1000 m the temperature rises to ~8.7°C at 200 m, 8.9°C at 500 m, and 9.0°C at 1000 m. The salinity reaches ~21.0 psu at 150 m, 21.4 psu at 200 m, 22.0 psu at 400 m, and 22.2 psu at 1000 m (Figure 4*b*). At 1000–1700 m, temperature and salinity increase slightly to 9.2°C and 22.35 psu, respectively. Thereafter, the temperature increase of 0.01°–0.02° to the bottom occurs as a result of geothermal heating, giving rise to development of a convective layer adjacent to the bottom. The bottom mixed layer, whose characteristics were explored in detail during the 1988 R/V *Knorr* cruises, occupies depths below 1700 m with uniform temperature and salinity values of 9.20°C and 22.35 psu, respectively [*Murray et al.*, 1991].

Density variations closely follow those of salinity (Figure 4*c*). However, the large seasonal temperature changes are reflected in the seasonal density variations in the uppermost 50 m layer (11.0–14.5 σ_t units). The density increases to 15.6 ± 0.2 at 100 m and 16.1 ± 0.1 at 150 m, so that the permanent pycnocline and permanent halocline are at the same depth. Below 200 m the density increases slowly, becoming 17.0 at 500 m and 17.2 at 1000 m, after which it increases only slightly to 17.23 at the bottom mixed layer.

3. HYDROGRAPHIC OBSERVATIONS

The meandering flow field along the Turkish coast was explored for the first time using modern data collection methods and closely spaced stations during four surveys conducted between 1987 and 1989. Two of these surveys (September 1988 and April 1989) covered both the eastern and western regions between approximately 28°E and 41°E. The April 1987 and January 1989 surveys covered only the western and eastern region, respectively. Details of the acquisition and processing of these survey data are given by *Oguz et al.* [1990].

The geopotential anomaly and sea surface temperature analyses of data taken during the R/V *Bilim* surveys are shown in Figures 5 and 6, respectively. As an aid in the discussions that follow, please refer to the bathymetric map of the Turkish coast in Figure 2.

Since most conductivity-temperature-depth (CTD) casts were carried out to 300-m depth, the dynamic computations used to derive the data for the geopotential anomaly analyses are based on a common reference level of 300 m. Since our aim is to describe the upper layer circulation, we consider this choice to adequately represent the baroclinic structure of the upper levels of the water column. Furthermore, it is also shallow enough to allow inclusion of most continental slope stations.

The sea surface temperature maps show that the surface thermal patterns generally follow the geopotential anomaly pattern. As a result, they are further evidence that the gradients in the satellite thermal imagery are indicative of

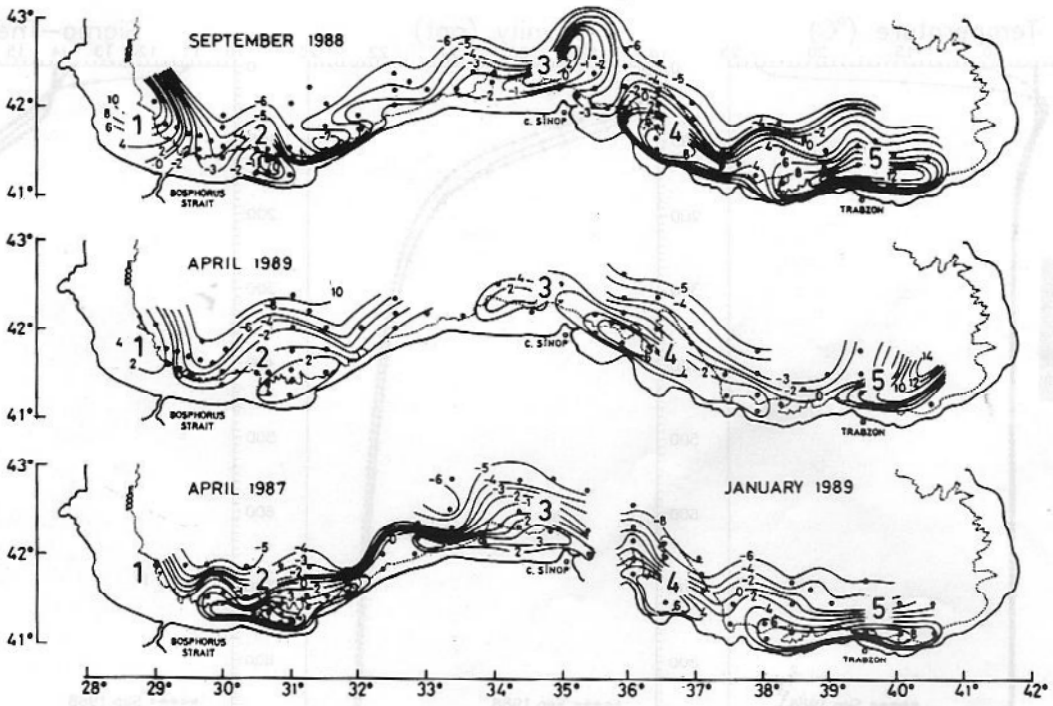

Fig. 5. Geopotential anomaly (10 m) maps for the R/V *Bilim* cruises conducted in April 1987, September 1988, January 1989, and April 1989. Note that to conserve space, the April 1987 and January 1989 data are shown together in the bottom figure. The large numbers indicate areas containing quasi-permanent features. These are also seen (but not numbered) in Figures 6, 7, 8, and 9.

current flow. The sea surface temperature maps will be used both in the hydrographic and satellite data discussions.

The geopotential anomaly and sea surface temperature maps for the August 26 to September 12, 1988, survey display flow and thermal patterns of a well-defined Rim Current flowing parallel to the coast. Entering the Bosphorus exit region from the north as a strong jet flow, the current follows the general topography associated with the Bosphurus Canyon and bifurcates into two branches (see *Oguz and Rozman* [1991] for further hydrographic evidence of the topographically driven flow in this region). While one branch continues to flow to the east, the other partially flows into

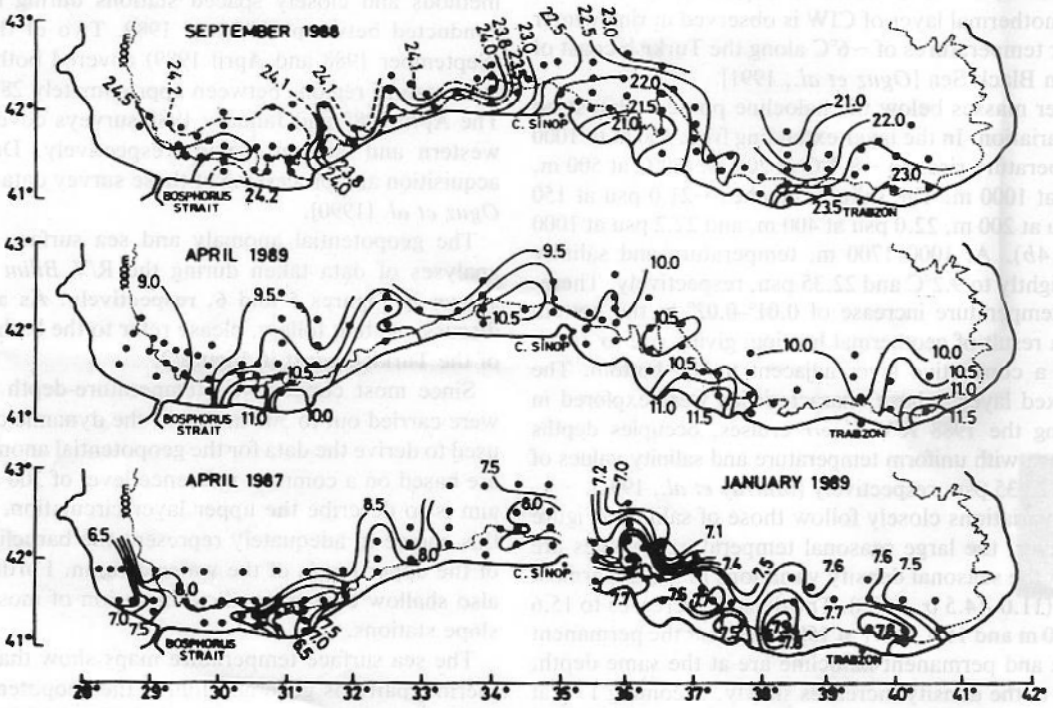

Fig. 6. Sea surface (10 m) temperature maps for the R/V *Bilim* cruises conducted in April 1987, September 1988, January 1989, and April 1989. Note that to conserve space, the April 1987 and January 1989 data are shown together in the bottom figure.

the Bosphorus and partially turns southwest to form an anticyclonic eddy northwest of the strait's entrance. This eddy is oriented parallel to the coast with its northern part located within Bulgarian coastal waters. The Bosphorus Eddy has been observed in this location during numerous hydrographic surveys [e.g., *Trukhchev et al.*, 1985; *Oguz and Rozman*, 1991]. As a further indication of its permanence, this structure is also visible in the April 1987 and April 1989 analyses as well as in the satellite imagery. Because of this permanence, we have named this eddy the Bosphorus Eddy. We will use this nomenclature of geographic names in naming the quasi-permanent eddies in the discussion that follows.

The eastern branch of the Rim Current turns offshore on the western side of the Bosphorus Canyon. From there it is redeflected toward the coast to again bifurcate and form an eddy over the Sakarya Canyon. We believe the actual topographic influence in this instant is not just the canyon, but also the ridge structure immediately to its west. For lack of a name for the ridge we will call this feature the Sakarya Eddy after the canyon. To the east of this feature, the cyclonic tendency of the flow, gained as it passes through the topographic trough, gives rise to intense upwelling at the coastal region. East of the Sakarya Eddy, the Rim Current is confined to the shelf break in the form of a strong meandering jet up to ~34°E.

Between 34°E and Cape Sinop, a strong elongated anticyclonic feature is formed that extends ~100 km in the offshore and the alongshore directions. Unfortunately, the hydrographic data from this cruise are insufficient to capture the offshore extent of what appears to be part of an eddy. The satellite data indicate that an eddy with a large cross-slope jet on its western side is often found at this location. Again, for discussion purposes and for lack of appropriate geographical name, we will call this feature the Sinop Eddy.

In the region between the Sakarya and Sinop eddies, the narrow shelf has colder temperatures than the interior basin. This relatively narrow zone of cooler water is probably associated with coastal upwelling caused by the persistent northeast winds which constitute the dominant regional wind regime found through most of the year.

Proceeding eastward into the Kizilirmak Canyon region, the Rim Current encounters the steep topographic slope to the east of the Yesilirmak Ridge and then continues to meander along the Eastern Black Sea Escarpment. Shoreward of the meandering flow, a large scale recirculating zone is formed consisting of two anticyclonic eddies. One of these, located between the coast and the Yesilirmak Ridge, seems to be topographically generated. The other, found between 38.5° and 41.0°E, constitutes the largest anticyclonic eddy formed along the Turkish coast. They will be referred to as the Yesilirmak and Trabzon eddies, respectively.

The Trabzon Eddy appears to be another quasi-permanent feature of the regional circulation, although its shape, strength, and orientation change in time [*Sorokin*, 1983; *Fashchuk and Ayzatullin*, 1986; *Novoselov et al.*, 1987]. This gyre is also apparent in Neumann's map (Figure 1*a*) as well as in the climatological mean surface dynamic topography map given by *Eremeev et al.* [1991]. In contrast to the apparent generating mechanisms of the other eddies, the presence of the Trabzon Eddy has been indicated to be related to local wind stress curl field that favor development of an anticyclonic eddy. This was indicated numerically by *Moskalenko* [1976], *Bulgakov and Korotaev* [1987], and *Stanev* [1988]. Details of their analyses, including the extremely important wind data, are not available. However, if the three studies are taken at face value, it appears as if local wind dependence is the cause for the comparatively large latitude of the pattern and position of this feature (i.e., greater than the other features we have discussed).

The cold surface temperatures of the Yesilirmak Eddy region seem influenced by input from local rivers (the Kizilirmak and Yesilirmak). However, the surface temperature distribution of the Trabzon Eddy reflects the normal situation of relatively warmer coast waters (implying neither wind-induced coastal upwelling nor river input).

The general features of the circulation do not change significantly with depth. The geopotential anomaly maps for the depths of 100 m and 200 m (not shown here) show patterns to the surface, albeit a somewhat weaker flow.

Features similar to those observed in the August–September 1988 analysis are also noticeable in the other analyses in Figures 5 and 6, indicating that they are possibly quasi-permanent. We have mentioned five distinct apparently quasi-permanent eddies in our discussion of the hydrographic data, marked by their corresponding numbers in Figure 5: the Bosphorus (1), Sakarya (2), Sinop (3), Yesilirmak, (4) and Trabzon (5) eddies. In our discussion of the satellite imagery that follows, features resembling the ones found in hydrographic analyses are marked by the same numerical identities.

4. SATELLITE OBSERVATIONS

The satellite imagery used in this study provided graphic information on the thermal and chlorophyll distribution in the Black Sea at the times of the satellite overpasses. The sea surface temperature and chlorophyll distributions are, of course, not direct current measurements. They can, however, depict the flow of the region in the manner the sea surface patterns of the hydrographic data followed that of the geopotential anomalies in Figures 5 and 6. The principal advantage of satellite data over ship data is the larger spatial extent and synoptic nature of the coverage. Barring obstructive cloud cover, unusually high humidity, and aerosols, their visible and thermal data can be made into imagery that will display patterns that can be used as tracers of the regional flow.

Detailed descriptions of the satellite sensors used in this study, the Nimbus Coastal Zone Color Sensor (CZCS) and a thermal channel of the NOAA Advanced Very High Resolution Radiometer (AVHRR), are found elsewhere [e.g., *Schwalb*, 1978; *Hussey*, 1979; *Hovis et al.*, 1980]. A number of papers discuss the oceanographic use of the NOAA AVHRR and Nimbus CZCS in the manner used here [e.g., *Arnone and La Violette*, 1986; *La Violette*, 1987], and the reader is referred to these papers for more complete information.

In essence, the Nimbus and NOAA satellites are polar-orbiting satellites, each of which is capable of sensing the Black Sea twice each day. In the case of the CZCS color imagery, an algorithm of two-channel data is used to remove the atmospheric effects and display the chlorophyll distribution. In the black and white images presented here, the lighter tones show greatest chlorophyll concentrations.

In the case of the thermal AVHRR, only channel 4 is used. The thermal imagery have not been atmosphericly corrected, only enhanced to show patterns related to the flow.

TABLE 1. Satellite Imagery Examined for This Study

Sensor	Dates
NOAA AVHRR	Feb. 1, 5, and 13, 1989
	April 4, 10, and 19, 1989
	May 2, 1989
	July 21, 22, 23, 24, and 26, 1989
	Aug. 1, 5, 6, 11, and 15, 1989
	Oct. 3, 8, 15, 21, 24, and 30, 1989
	Nov. 7 and 21, 1989
	Dec. 5, 9, 14, 18, and 22, 1989
	Jan. 12, 14, 21, 25, and 26, 1990
	Feb. 27, 1990
	March 8, 1990
	June 17 and 20, 1990
	Aug. 29, 1990
Nimbus CZCS	June 12, 13, and 14, 1980
	July 7, and 22, 1980
	Aug. 13, 14, 21, 23, and 29, 1980
	Sept. 9 and 11, 1980
	Oct. 13, 1980
	May 10, 21, and 24, 1981
	June 16 and 24, 1981
	July 3 and 19, 1981
	Aug. 7 and 8, 1981
	Sept. 7, 1981
	May 5, 10, and 17, 1982
	Aug. 21, 1982
	Sept. 12, 1982

In the thermal imagery the lighter tones represent the warmer waters. The darkest portions in both types of imagery are clouds. All of the imagery is registered to a Mercator projection.

Table 1 presents the imagery examined for this study. Despite the somewhat limited number of images available to us (40 AVHRR and 28 CZCS), they were sufficient to provide a detailed spatial display of the circulation patterns indicated by the hydrographic data as well as an idea of their permanence (as far as location is concerned) and prevalence (as far as current pattern is concerned). Although the whole sea will be discussed, the emphasis will be on characteristics of the southern shelf and slope area so as to allow comparison with the R/V *Bilim* hydrographic data. As will be shown, the imagery reveals structural similarity with the flow patterns inferred earlier from the hydrographic data.

Few of the images examined were more than 50% free of clouds. We have presented several examples of the more cloud-free imagery in Figure 7 (see also Figure 1*b*) in an attempt to show representative conditions for various periods of the data set. This sampling (as well as the complete imagery set) indicates that the interior of the Black Sea has a more complex circulation than is indicated in Neumann's analysis in Figure 1*a*. The winter thermal imagery indicates a possibly stronger shelf circulation than that in summer. The early winter (i.e., prior to February) Rim Current and associated coastal eddies are larger and more pronounced and the thermal gradients much stronger than those seen in the other seasonal imagery (e.g., compare the December 18, 1989, image in Figure 1(b) with the February 27, 1990, image in Figure 7*a*. This is also noticeable in the historical sea surface temperature data which show the summer gradients are weaker than the early winter gradients (Table 2).

The chlorophyll distribution in the Nimbus CZCS imagery shows patterns similar to the thermal imagery except that (as would be expected from chlorophyll imagery) patterns are as well defined in summer as in winter. The full-resolution CZCS image for 1982 in Figure 7*e* shows a feature in much the same position as the jetlike structure located west of Cape Sinop in the 1989 time series in Figure 8.

All the cloud-free images that included the western portion of the sea show the influence of the Danube and regional coastal rivers with a flow of cold, low-salinity water that moves southward along the western shelf (e.g., the February and May images in Figures 7*a* and 7*b*). As this shallow flow moves to the south, it remains close to shore, maintaining a jetlike flow, and is separated by the Rim Current and the general circulation of the western basin by a pronounced temperature front. As the jet encounters the southern shelf, the coastal fresh water gradually looses its identity by mixing with the Rim Current water in the region of the Bosphorus Eddy (eddy 1).

As the flow moves eastward it forms the meanders and eddies noted in the hydrographic data. Although showing some changes in shape and size, many of the features appear in both the thermal and color imagery in the same general location throughout the year.

As the flow moves along the Turkish coast, almost all of the images display numerous jets and filaments, often with dipole eddies at their termina extending from the shelf into the offshelf waters. The importance of this type of flow in the coastal–deep basin exchange is indicated in studies of other regions showing similar phenomena. For example, turbulent filaments and eddies associated with the California Current system have been identified as crucial to the regional cross-shore transport [*Mooers and Robinson*, 1984]. Similar work has been done to derive the circulation structure of multiple dipole eddies in the Alaska coastal current [*Ahlnäs et al.*, 1987] and in the Balearic Sea [*Wang et al.*, 1988; *Tintoré et al.*, 1990; *La Violette et al.*, 1990].

Analysis of successive images available for this study showed no indication of feature translation, and the major features which are clearly represented in repeated images appeared stationary. For example, an examination of daily imagery of the jet situated just west of Cape Sinop for 25 days showed no eastward movement. Samples of these data in Figure 8 shows there was obvious deformation of the feature during the period but that it did not move from its initial reported position. However, this appearance of non-translation may be due to the slow translation rate of the features (~2–3 cm/s [*Latun*, 1990]) and the limited continuous temporal series available for the study. Note also that the Sinop Eddy immediately east of the jet showed vigorous rotation but no eastward translation.

One exceptional feature immediately noticeable in our examination of the satellite thermal imagery set is the seasonal reversal of the coastal and deepwater temperature gradients. We found the coastal waters are warmer than the central waters in early winter (i.e., before February). In summer, although the gradients are much weaker, the coastal waters are cooler and show definite upwelling characteristics. A casual examination of imagery for years other than 1989–1990 indicates that this may be a normal variation.

The thermal imagery available for this study is insufficient to allow a positive demarcation as to when this reversal takes place during the year. Note, however, that the thermal reversal can also be seen in the historical sea surface temperature data in Table 2. These show that during September through January, the coastal waters are at least 0.5°C

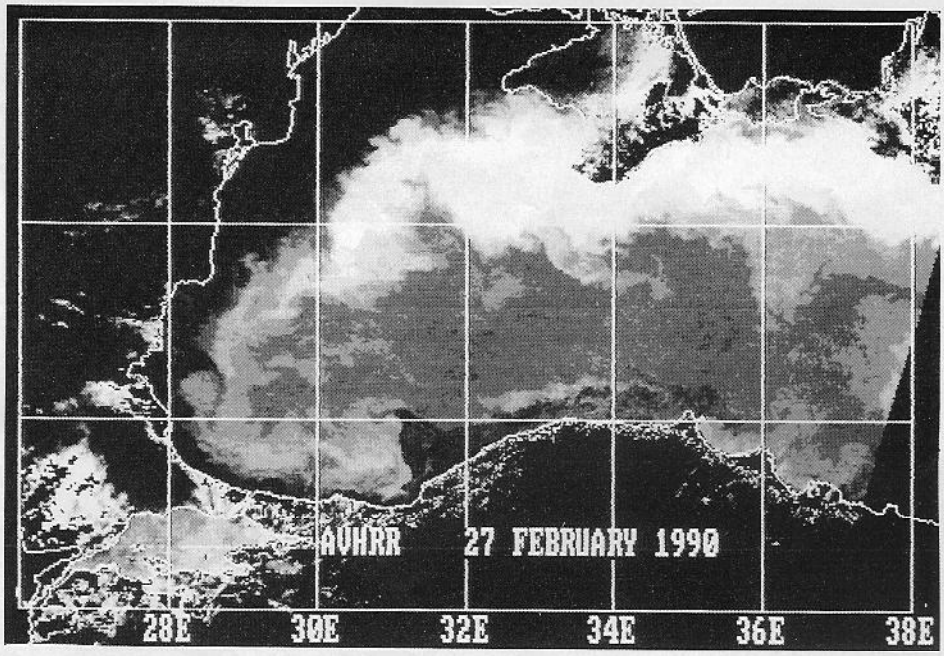

Fig. 7*a*

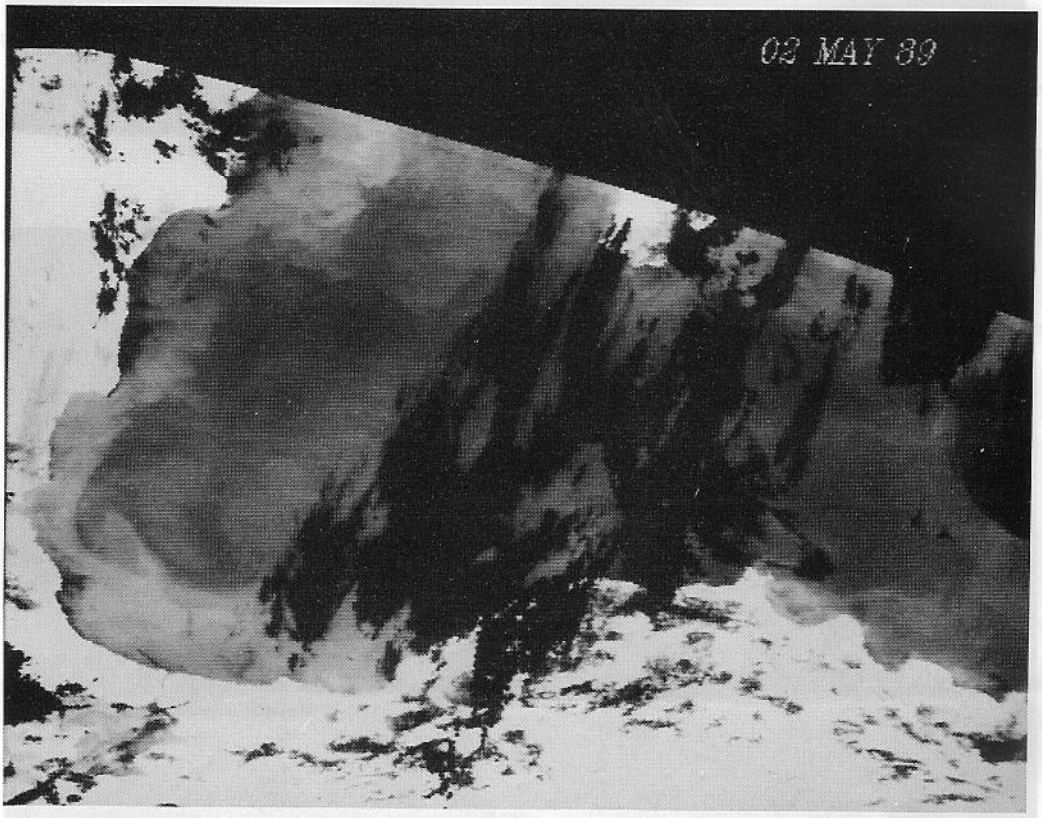

Fig. 7*b*

Fig. 7. Representative 2-km resolution Mercator-registered NOAA AVHRR thermal imagery from (*a*) February 27, 1990, (*b*) May 2, 1989, (*c*) July 24, 1989, (*d*) October 24, 1989, and (*e*) representative Nimbus 7 CZCS imagery from July 19, 1980.

warmer than the central basin. These are the same months indicated by the satellite thermal imagery.

In the region between the Sakarya and Sinop eddies (eddies 2 and 3) the satellite and hydrographic data indicate a narrow cold band of evidently upwelled water. We have looked at just this region in the historical data and also found it to be colder than the interior basin.

It should be mentioned that the historical sea surface

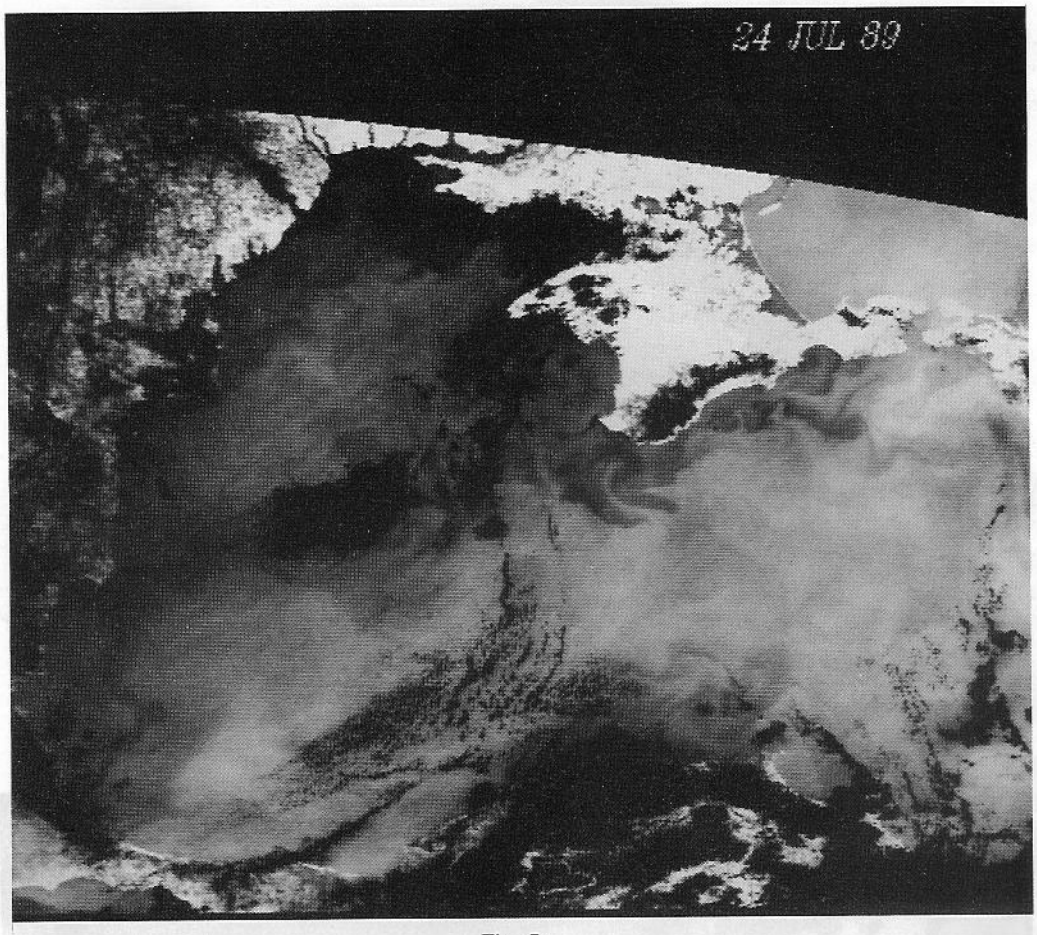

Fig. 7*c*

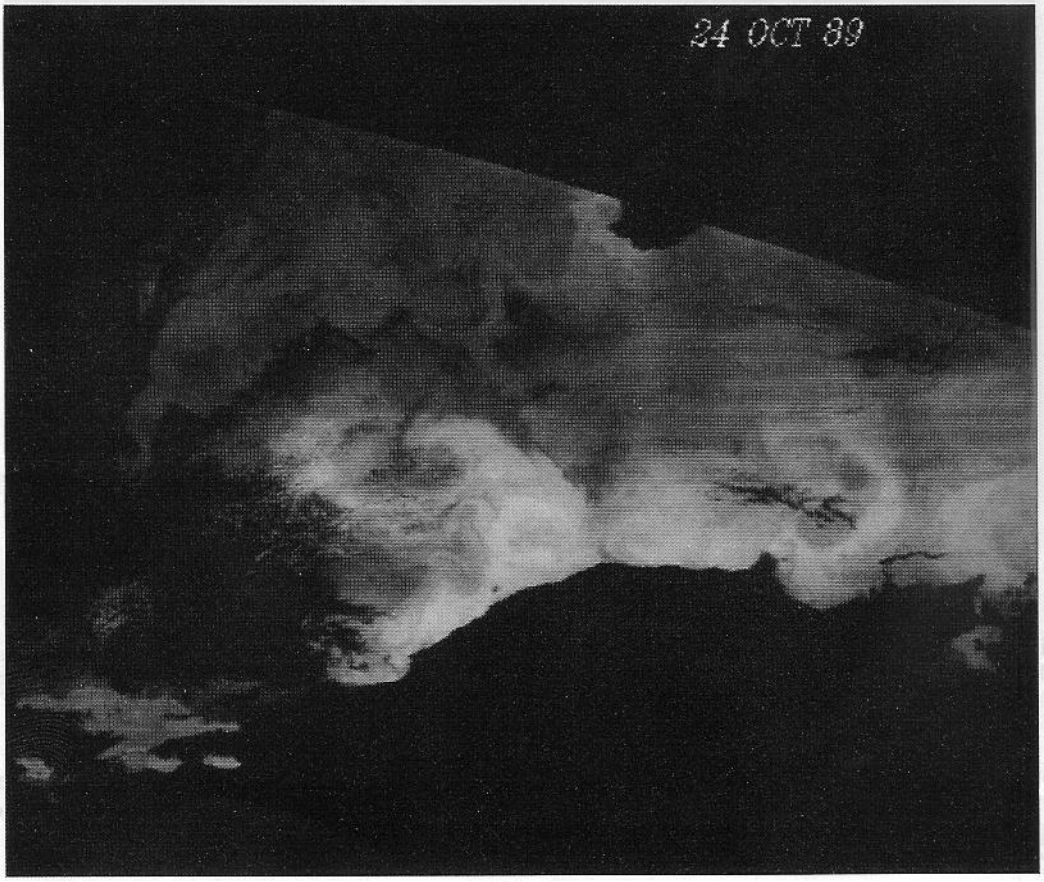

Fig. 7*d*

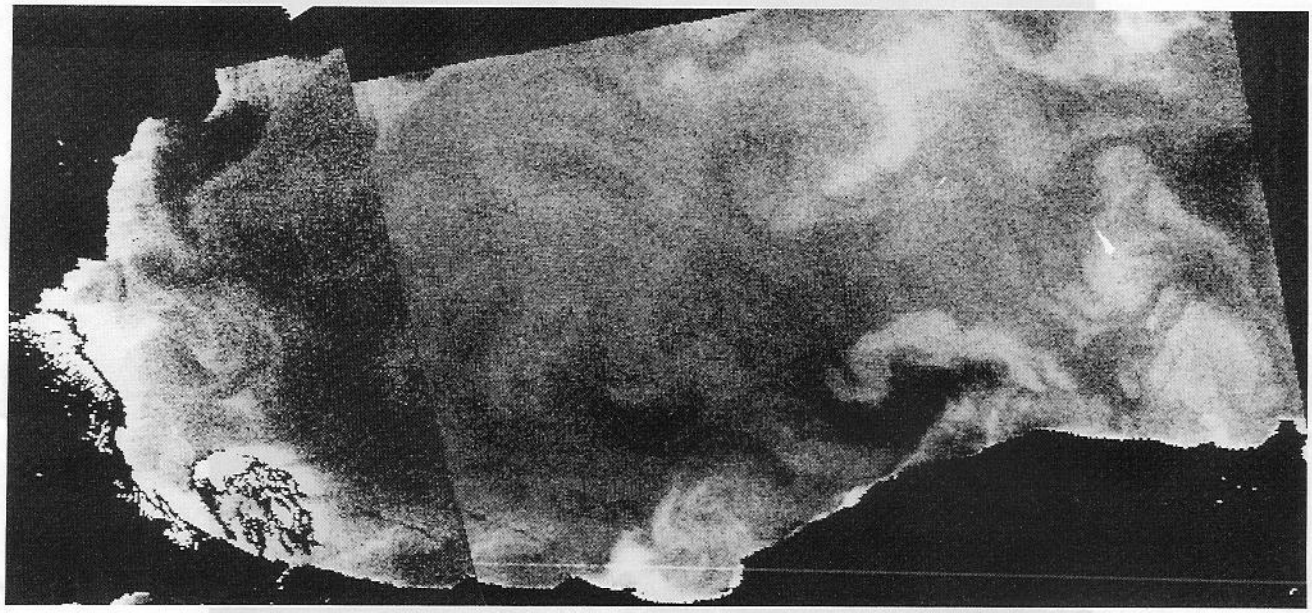

Fig. 7e

temperatures are based on long-term averages plotted on an ~0.75° latitude-longitude grid. This averaging over such a coarse grid smoothes the seasonal coastal–central basin gradients, and (as is indicated by the satellite imagery) it is likely that they are much stronger than the gradients presented in the table.

If we accept the central doming hypotheses expounded by such investigators as *Blatov* [1984], then it may be suggested that the reversal is caused by the seasonal variation in flow in the interior. That is, that the relatively cooler interior water in winter is due to the doming structure associated with the cyclonic character of the flow, and this is separated from the advecting differing density coastal water by a well-pronounced frontal structure (This will be discussed further in section 5).

In February and March, both the satellite imagery and the historical sea surface temperatures data indicate that the temperature in the central basin and coastal south areas is more uniform, indicative of the eventual cooling and mixing of the coastal waters.

TABLE 2. Monthly Variations of the Mean Sea Surface Temperatures (SST) for Selected Areas of the Black Sea

	Region*				
Month	WB	TC	WC	EC	SS
Jan.	8.6	9.5	8.7	9.0	8.7
Feb.	7.1	7.7	7.3	7.6	7.3
March	7.2	7.5	7.7	7.2	7.4
April	9.6	9.7	9.7	9.8	9.5
May	14.5	14.4	13.5	15.0	14.0
June	19.6	19.3	19.1	20.1	19.0
July	23.0	23.1	23.1	23.9	22.5
Aug.	23.7	24.0	23.5	24.3	23.0
Sept.	21.4	21.9	20.9	21.0	21.2
Oct.	17.8	18.7	17.4	17.6	18.0
Nov.	14.2	15.0	13.8	14.0	14.7
Dec.	11.3	12.0	11.1	11.0	11.5

After *Altman et al.* [1987].

*Abbreviations are as follows: WB, SST averaged for whole basin; TC, SST averaged along the Turkish coastal zone; WC, SST averaged for the central part of the western basin; EC, SST averaged for the central part of the eastern basin; SS, SST averaged for the coastal region between the Sakarya and Sinop eddies along the Turkish coast.

5. DISCUSSION

Because of sparsity and spacing of ocean stations, early studies of the Black Sea presented a simple pattern of a single- or dual-dome circulation. However, our analysis of satellite and closely spaced hydrographic observations indicate a sea with complex basin-wide cyclonic circulation system and multiple scales of motion.

Our analysis indicates that the Black Sea has three regimes of flow, each having descending order of scaler magnitude in the circulation. These are (1) the Rim Current and central circulation, (2) topographic and local strong wind-induced semipermanent variations, and (3) frontal instabilities and small scale wind changes. We will discuss these regimes in this order.

Rim Current and Central Basin Circulation

As was indicated earlier, the major forcing of the circulation, the wind stress curl, results in the sea having a general cyclonic circulation. For example, the numerical analysis of *Moskalenko* [1976] showed that the wind stress curl field operating on a homogeneous Black Sea of constant depth with the planetary beta effect results in a peripheral current with two nodal centers (Figure 9). The effects presented were for conditions in winter the period having the stronger wind conditions. The weaker winds of summer are inferred to result in less coherent current patterns.

Although Moskalenko did show the effects of the bathymetry as part of his results, neither his method of inclusion nor scale of resolution was documented, and his results appear too simplistic to show the effect of the bottom topography or even major coastal shapes beyond the broad restriction of the polygon in Figure 9.

If the effects of topography are more realistically considered, we believe the topography will act as a modifier of the

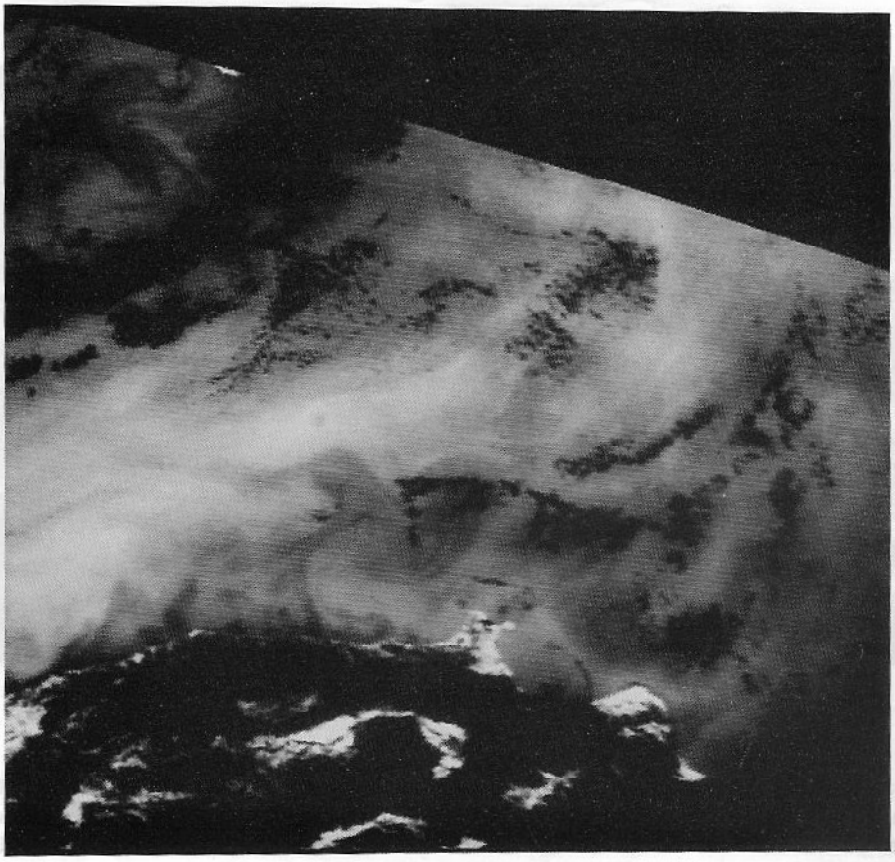

Fig. 8*a*

Fig. 8*b*

Fig. 8. Full-resolution (1 km), Mercator-registered NOAA AVHRR thermal images of the Turkish coast for (*a*) July 22, (*b*) August 1, (*c*) August 6, and (*d*) August 15, 1989, showing a cool jet extending from the Turkish coast that was monitored by the satellite from July 23 through August 16 1989. Note the series of dipole eddies shed by the plume that extend deep into the central basin.

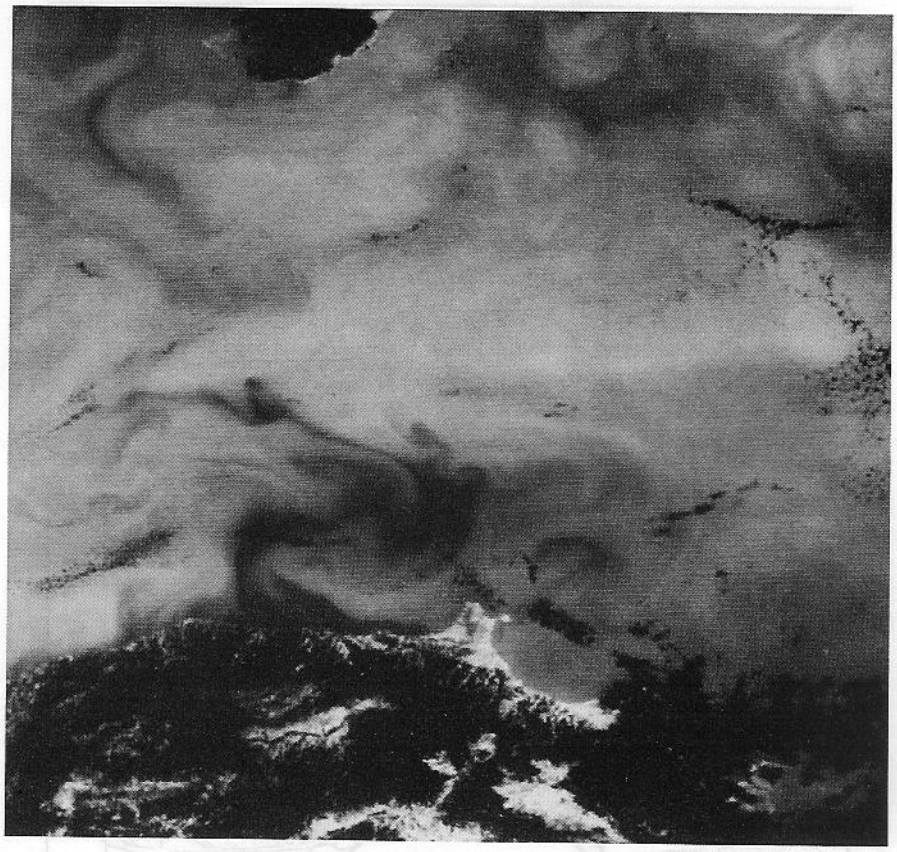

Fig. 8*c*

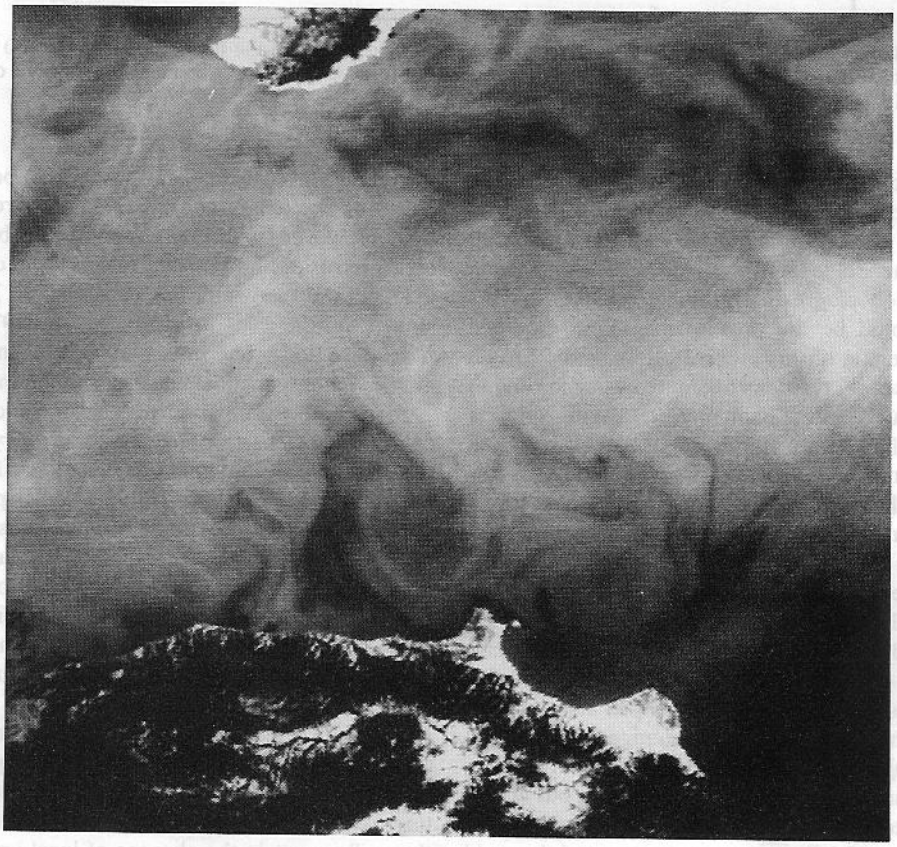

Fig. 8*d*

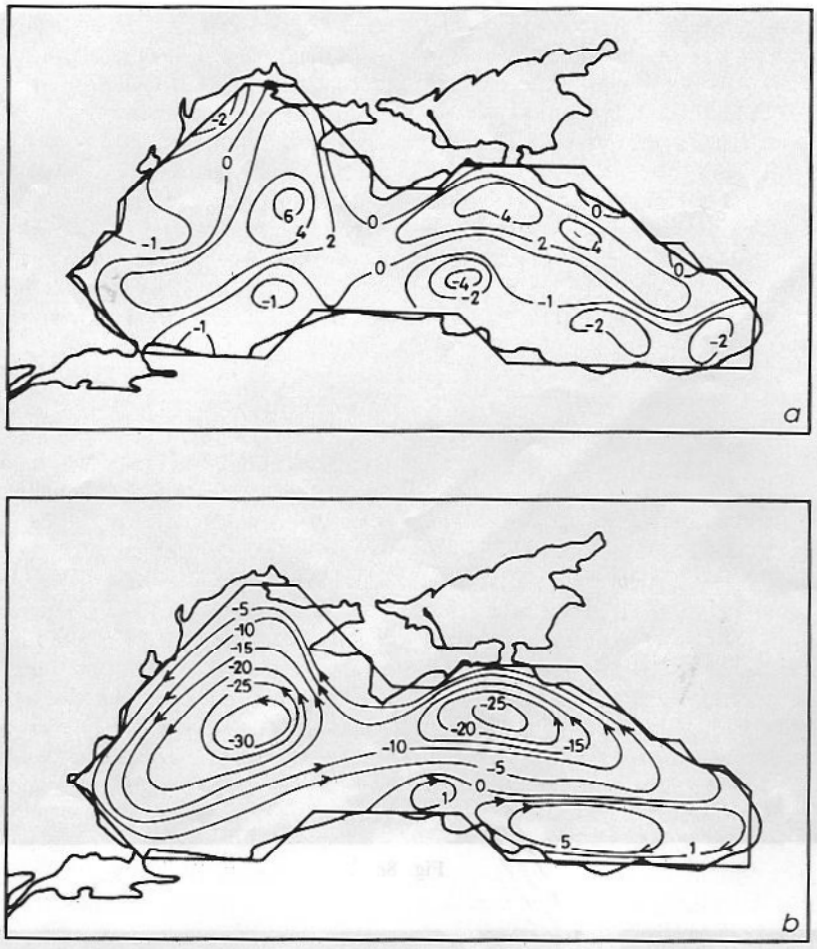

Fig. 9. (*a*) The climatological mean winter wind stress curl field pattern in the Black Sea in units of 10^7 dyn/cm^3. (*b*) The total transport stream function of steady state wind-driven currents for a homogeneous ocean of constant depth in units of 10^2 cm^3/s [*Moskalenko*, 1976].

wind curl circulation that should change the speed of the current directly over the region of sharpest gradient due to the contribution of the topographic beta effect. The result would be that in the Black Sea, the rim of the continental shelf (i.e., the region of greatest gradient change) and its downslope side would be the area of maximum modified current flow. The region of this modified flow would form a ribbon around the sea that widens and narrows according to the slope area. Our limited examination of the satellite imagery indicates that such a ribbon exists (albeit modified by smaller-scale conditions we will discuss shortly). It is this ribbon we have called the Rim Current.

The winter generation of CIW creates a density pattern which adds to the distinct character of the Rim Current. When (and wherever) CIW is generated, its shelf component is advected by the Rim Current around the periphery of the sea. Although modified as it is advected, the water mass retains its density contrast between the shelf and interior waters. These cross-shelf density changes will also contribute to flow variation. Examples of such changes are given by *Tintoré et al.* [1990] and *La Violette et al.* [1990].

There also appears to be thermohaline forcing, but at this time it is difficult to separate the effects of this secondary forcing from the effect of the stronger wind stress curl. It would appear that the major thermohaline contribution would be limited to the upper layer (because of the density restriction of the permanent halocline) and would be a positive effect on the flow with the winter current being the stronger seasonal current. However, without information on buoyancy, displacement, intrusion, and mixing effects, it is difficult to do more than surmise the wintertime contribution. In numerical model studies of the sea, *Marchuk et al.* [1975], *Bulgakov and Korotaev* [1987], and *Stanev* [1988, 1990] noted the secondary but not inconsequential effect of the thermohalinic forcing.

A possible explanation for the presence of the relatively colder narrow coastal zone between Sakarya and Sinop eddies observed in our September 1988 and April 1987 hydrographic data is upwelling caused by year-round prevailing northeast winds. In the summer months, such winds cause upwelling of the CIW with temperatures of 7°–8°C across the seasonal thermocline. This upwelling-induced mixing of two water masses having considerable temperature difference leads to an appreciable reduction in the surface temperature. Although upwelling-favorable northeast winds continue during the winter months, the surface and subsurface CIW waters have almost the same temperature values, and the sea surface temperature patterns do not show the upwelling process as clearly as in summer. The typical winter sea surface temperatures distribution along the shelf will then be similar to the one that will appear in the absence of local upwelling; i.e., colder interior and slightly warmer coastal waters associated with the cyclonic general circulation of the basin.

Note that the thermal and visible features seen in the satellite imagery do not infer a well-defined flow structure in the central region as along the coasts. Instead, the flow is indicated to be weak and diffused with no central loci. In fact, the double doming shown in Figure 1*a* is not noticeable in any of the images examined. However, if there were a broad comparatively weak central upwelling, the surface currents might not show such a well-defined flow pattern. In our opinion, the results are inconclusive for either case. What is apparent is that in both summer and winter, the circulation is indicated to be variable, with multiple small eddies and long filaments with no particular orientation that may reach as long as 100 km.

Topographic Control and Local Strong Wind-Induced Semipermanent Circulation

Imposed on the seasonally variable Rim Current and central basin circulation are modifications induced by prominent topographic features and transient (several weeks) strong winds (of the order of 10 m/sec). We have noted that along the Turkish coast, the Rim Current might be modified by its interaction with specific bathymetric features in at least two instances (eddies 2 and 4), and an apparent local wind generated feature at another instance (eddy 5). The Rim Current enters the Bosphorus exit region in the form of a well-defined jet flow and splits into two branches. One branch enters partially into the Bosphorus Strait and eventually forms the relatively fresh upper layer waters of the Turkish straits system. The remaining part turns anticyclonically in the northwesterly direction forming an anticyclonic eddy on the Bulgarian shelf. It seems that the intensity of flow deflected southward outside the Bosphorus Strait varies in time and regulated by the transport capacity of the Rim Current. (It is apparent that the Bosphorus Eddy exerts a strong influence on the characteristics of the water entering the Bosphorus Strait. Thus it is important in the broader context of the interaction of the Black Sea and Mediterranean Sea, i.e., on the water entering the Mediterranean and, as a result of exchanges taking place within the strait, on waters entering the Black Sea).

The second branch of the rim current proceeds eastward, following the local topography along the continental slope comprising the depth interval 200–2000 m, and forms a series of anticyclonic eddies. The Sakarya and Yesilirmak eddies (eddies 2 and 4) appear to be controlled by the complex regional topography.

Topographic control of the Rim Current in the Black Sea is noted quantitatively by the numerical model studies [e.g., *Bulgakov and Korotaev*, 1987; *Stanev*, 1988, 1990]. Introducing realistic basin topography and using the climatological mean winds and density fields, the computed circulation patterns show the meandering currents and a series of mesoscale eddies around the periphery of the sea. For example, the current field obtained by *Bulgakov and Korotaev* [1987] shows coastal features similar to these described earlier using the hydrographic data.

Frontal Instabilities and Small-Scale Wind Forcing

The satellite imagery indicates mesoscale and submesoscale variability which appears to have been induced by instabilities associated with both horizontal and vertical shears in the flow as well as horizontal gradients between coastal and interior waters. The role of the instability mechanisms on the meandering Rim Current was demonstrated in the numerical experiments carried out by *Stanev* [1988, 1990]. In addition, the wind regime appears to go counter to the flow and near the coast is sufficient to create a counter circulation which produces small-scale upwelling.

The results show that the boundary current system along the Turkish coast possesses meanders with offshore extent of ~75 km from the shelf break and with longshore wavelengths of 100–150 km. The form of the instantaneous flow field gives evidence for the combined effects of topographic irregularities and instabilities mechanisms. It appears that small-amplitude meanders are initiated by alongshore topographic irregularities and transient winds. The meanders then grow into larger-amplitude meanders in time owing to instability processes and eventually may become detached from the flow [*Ikeda et al.*, 1984, 1989; *Chao*, 1990]. For example, the form of the isolines east of Sakarya Eddy shown in Figure 5 seems to depict a situation before a detachment process. This is apparent from the filamentary feature associated with the backward curling of the flow.

The mesoscale eddies and other fine structure details (fronts, filaments, fluctuations) act as interaction media within the flow field, generating a highly energetic and temporally variable circulation. Our examination of satellite imagery has shown numerous circulation patters in other portions of the sea that are similar to the five features noted along the Turkish coast. We believe that this type of interactions is typical of the sea and that similar combined studies will produce multiple examples of a similar nature.

6. CONCLUSIONS

The observations reported here describe, for the first time, the mesoscale variability along the southern periphery of the Black Sea. Our particular concern in this exploratory study is to examine existing complex temporal and spatial variability of the region's dynamical processes and thereby form a basis for the methodology of future experimental and theoretical studies in the Black Sea. Our aim is to achieve ultimately a thorough understanding of the underlying dynamics. The study shows the necessity of future investigations with two primary objectives: (1) to obtain definitive and comprehensive data set with sufficient resolution that will serve as the data base for the understanding of the dynamics of the Black Sea, particularly providing information on the variability and the energetics of the general circulation, subbasin and mesoscale flows, convection and water mass formation and spreading, and (2) to construct a hierarchy of multiple-scale realistic models that would have components of regional processes and general circulation and be suitable for application to climatological, biological, and chemical studies.

Since the Black Sea is geographically constrained, it may serve as a small-scale laboratory for investigation of a series of phenomena that are common to different areas of the world ocean.

Acknowledgments. The main part of this work was carried out under the sponsorship of NATO Science for Stability Program. Partial support was provided by the Turkish Scientific and Technical Research Council (TUBITAK) and Mississippi State University Research Center. The encouragement and support given by the Director of the NATO Science for Stability Program for establishing

the satellite image processing system in the Middle East Technical University, Erdemli Institute of Marine Sciences, Turkey, are greatly acknowledged. We also wish to thank the anonymous reviewers for their constructive remarks.

REFERENCES

Ahlnäs, K., T. C. Royer, and T. H. George, Multiple dipole eddies in the Alaska Coastal Current detected with Landsat thematic mapper data, *J. Geophys. Res.*, *92*(C12), 13,041–13,047, 1987.

Altman, E. N., I. F. Gertman, and Z. A. Golubeva, Climatological fields of temperature and salinity in the Black Sea (in Russian), *Rep. 115*, 111 pp., Sevastopol Branch, State Oceanogr. Inst., Sevastopol, Ukraine, 1987.

Arnone, R. A., and P. E. La Violette, Biochemical properties of the North African Current, *J. Geophys. Res.*, *91*(C2), 2351–2364, 1986.

Blatov, A. S., A. N. Kosarev, and V. S. Tuzhilkin, Variability of the hydrographic structure of the Black Sea water and its links with external factors (in Russian), *Vodn. Resur.*, *6*, 71–82, 1984.

Bogatko, O. N., S. G. Boguslavskiy, M. Beljakov, and R. E. Ivanov, Surface currents in the Black Sea, in *Complex Studies of the Black Sea* (in Russian), pp. 26–33, Marine Hydrophysic Institut, Sevastopol, Ukraine, 1979.

Bulgakov, S. N., and G. K. Korotaev, Diagnostic calculation of the Black Sea climatic circulation on full nonlinear model (in Russian), *Morsk. Gidrofiz. Zh.*, *2987*(1), 7–13, 1987.

Caspers, H., Black Sea and Sea of Azov, in Treatise on Marine Ecology and Paleoecology, edited by J. W. Hedgpet, *Mem. Geol. Soc. Am.*, *67*(1), 801–890, 1957.

Chao, S.-Y., Instabilities of fronts over a continental margin, *J. Geophys. Res.*, *95*(C3), 3199–3211, 1990.

Eremeev, V., V. Ivanov, A. Kosarev, and V. Tuzulkin, Climatic interannual variability of geostrophic circulation in the Black Sea, *Sov. J. Phys. Oceanogr.*, in press, 1991.

Fashchuk, D. Y., and T. A. Ayzatullin, A possible transformation of the anaerobic zone of the Black Sea, *Oceanology*, Engl. Transl., *26*(2), 171–178, 1986.

Hovis, W. A., D. L. Clark, F. Anderson, R. W. Austin, W. H. Wilson, E. T. Baker, D. Ball, H. R. Gordon, and J. L. Muller, Nimbus-7 CZCS: System description and initial imagery, *Science*, *210*, 60–63, 1980.

Hussey, W. J., The Tiros-N/NOAA Operational Satellite System, *NOAA NESS Tech. Memo. 95*, 35 pp., Natl. Environ. Satell. Data Inf. Serv., Natl. Oceanic Atmos. Admin., Washington, D. C., 1979.

Ikeda, M., L. A. Mysak, and W. J. Emery, Observation and modelling of satellite-sensed meanders and eddies off Vancouver Island, *J. Phys. Oceanogr.*, *14*, 3–21, 1984.

Ikeda, M., J. A. Johannessen, K. Lygre, and S. Sandven, A process study of mesoscale meanders and eddies in the Norwegian Coastal Current, *J. Phys. Oceanogr.*, *19*, 20–36, 1989.

Knipovich, N. M., The hydrological investigations in the Black Sea (in Russian), *Tr. Azovo Chernomorsk. Nauchnopromysl. Eksped.*, *1932*, no. 10, 274 pp., 1932.

Latif, M. A., E. Ozosy, T. Oguz, and U. Unluata, Observations of the Mediterranean effluent in the Black Sea, *Deep Sea Res.*, *38*, suppl. 2, 5711–5723, 1991.

Latun, V. S., Anticyclonic eddies in the Black Sea in summer 1984 (in Russian), *Sov. J. Phys. Oceanogr. 1*(4), 279–286, 1990.

La Violette, P. E., Satellite image analysis techniques applied to oceanography, *Philos. Trans. R. Soc. London, Ser. A*, *324*, 325–346, 1987.

La Violette, P. E., J. Tintoré, and J. Font, The surface circulation of the Balearic Sea, *J. Geophys. Res.*, *95*(C2), 1559–1568, 1990.

Marchuk, G. I., A. A. Kordzade, and Yu. N. Skiba, Calculation of the basic hydrological fields in the Black Sea, *Izv. Acad. Sci. USSR Atmos. Oceanic Phys.*, Engl. Transl., *11*(4), 379–393, 1975.

Mooers, C. N. K., and A. R. Robinson, Turbulent jets and eddies in the California Current and inferred cross-shore transports, *Science*, *223*, 51–53, 1984.

Moskalenko, L. V., Calculation of stationary wind-driven currents in the Black Sea, *Oceanology*, Engl. Transl., *15*(2), 168–171, 1976.

Murray, J. W., Z. Top, and E. Ozsoy, Hydrographic properties and ventilation of the Black Sea, *Deep Sea Res.*, *38*, suppl. 2, 663–690, 1991.

Neumann, G., Die absolute Topografie des physikalischen Meeresniveaus und die Oberflachen-Stromungen des Schwarzen Meeres, *Ann. Hydrogr. Berlin*, *70*, 265–282, 1942.

Novoselov, A. A., Ye. Ye. Sovga, D. Ya. Fashchuk, S. M. Khomutov, and A. I. Sheremet'yeva, Comparative evaluation of the iodometric and fluorometric methods of determining hydrogen sulfide in the layer of its coexistence with oxygen in the Black Sea, *Oceanology*, Engl. Transl., *27*(3), 304–307, 1987.

Oguz, T., and L. Rozman, Characteristics of the Mediterranean underflow in the southwestern Black Sea continental shelf/slope region, *Oceanol. Acta*, *14*(5), 433–444, 1991.

Oguz, T., S. Tugrul, F. Bingel, and M. Unsal, Stock assessment studies for the Turkish Black Sea coast, *NATO-TU Fish. Tech. Rep.*, *1*, 122 pp., NATO Sci. for Stability Programme, Inst. of Mar. Sci., Middle East Tech. Univ., İçel, Turkey, 1990.

Oguz, T., M. A. Latif, H. I. Sur, E. Ozsoy, and U. Unluata, On the dynamics of the southern Black Sea, in *The Black Sea Oceanography, NATO ASI Ser.*, edited by J. W. Murray and E. Izdar, pp. 43–64, Kluwer Academic, Norwell, Mass., 1991.

Ovchinnikov, I. M., and Yu. I. Popov, Evolution of the cold intermediate layer in the Black Sea, *Oceanology*, Engl. Transl., *27*(5), 555–560, 1987.

Ozsoy E., Z. Top, G. White, and J. W. Murray, Double diffusive intrusions, mixing and deep sea convective precesses in the Black Sea, in *The Black Sea Oceanography, NATO ASI Ser.*, edited by J. W. Murray and E. Izdar, pp. 17–42, Kluwer Academic, Norwell, Mass., 1991.

Paramonov, A. N., O. B. Zakharova, and S. I. Chernoinanov, A possible source of formation of Black Sea cold intermediate layer (in Russian), *Morsk. Gidrofiz. Zh.*, *1988*(5), 61–64, 1988.

Schwalb, A., The Tiros-N/NOAA A-G satellite series, *NOAA Tech. Memo. NESS 95*, 75 pp., Natl. Environ. Satell. Data Inf. Serv., Washington, D. C., 1978.

Sorokin, Yu. I., The Black Sea, in *Estuaries and Enclosed Seas, Ecosystems of the World*, vol. 26, edited by B. H. Ketchum, pp. 253–292, Elsevier, New York, 1983.

Stanev, E., Numerical study on the Black Sea circulation, *Mitt. Inst. Meereskd. Univ. Hamburg*, *28*, 232 pp., 1988.

Stanev, E., Numerical modelling of the circulation and the hydrogen sulfide and oxygen distribution in the Black Sea, *Deep Sea Res., Part A.*, *36*(7), 1053–1065, 1989.

Stanev, E. V., On the mechanism of the Black Sea circulation, *Earth Sci. Rev.*, *28*, 285–319, 1990.

Tintoré, J., D. Wang, and P. E. Violette, Eddies and thermohaline intrusions of the shelf/slope front off the northeast Spanish Coast, *J. Geophys. Res.*, *95*(C2), 1627–1634, 1990.

Titov, V. B., Velocity distribution of surface current in the vicinity of the North Caucasus coast of the Black Sea, *Oceanology*, *25*(3), 314–318, 1985.

Tolmazin, D., Changing coastal oceanography of the Black Sea, I, Northwestern shelf, *Prog. Oceanogr.*, *15*, 217–276, 1985*a*.

Tolmazin, D., Changing coastal oceanography of the Black Sea, II, Mediterranean effluent, *Prog. Oceanogr.*, *15*, 277–316, 1985*b*.

Trukhchev, D. I., Ye. V. Stanev, G. D. Balashov, G. D. Miloshev, and V. M. Rusenov, Some unique features of the mesoscale structure of hydrological fields in the western part of the Black Sea, *Oceanology*, *25*(4), 443–446, 1985.

Unluata, U., and P. E. La Violette, Eddies and filaments associated with the coastal circulation of the Black Sea (abstract), *Eos Trans. AGU*, *71*(2), 135, 1990.

Unluata, U., T. Oguz, M. A. Latif, and E. Ozsoy, On the physical oceanography of the Turkish straits, in *The Physical Oceanography of Sea Straits, NATO ASI Ser.*, edited by L. J. Pratt, pp. 25–60, Kluwer Academic, Norwell, Mass., 1990.

Wang, D. P., M. Viera, J. Salat, J. Tintoré, and P. E. La Violette, A shelf slope frontal filament off the northeast Spanish coast, *J. Mar. Res.*, 321–332, 1988.

Yuce, H., Investigation of the Mediterranean water in the Strait of Istanbul (Bosphorus) and the Black Sea, *Oceanol. Acta.*, *13*(2), 177–186, 1990.

P. E. La Violette, Mississippi State University Research Center, Stennis Space Center, MS 39529.

T. Oguz and U. Unluata, Institute of Marine Sciences, Middle East Technical University, P. O. Box 28, Erdemli 33731, İçel, Turkey.

(Received June 18, 1991;
accepted December 12, 1991.)